JSER

Journal of Solar Energy Research (JSER)

Journal homepage: www.jser.ut.ac.ir

Experimental Study of Nanoparticles-Coated Solar Photovoltaic Modules: Energy and Exergy Enhancement

Ahmed Khudhur, Hussein Jobair*

Department of Energy Engineering, College of Engineering, University of Baghdad, Baghdad, Iraq

ARTICLE INFO

Article Type:

Research article

Received:2026.06.14
Accepted in revised form:2026.07.05

Keywords:
Solar energy; PV module; Nanocoatings; Energy efficiency; Exergy efficiency

A B S T R A C T

This study experimentally investigates the effect of TiO_2 and SiO_2 nanocoatings on the photovoltaic (PV) modules performance under Baghdad, Iraq, climatic conditions. Three identical monocrystalline PV modules; an uncoated reference module and two nanocoated modules, were tested under real outdoor conditions during three separate experimental days. The effects of solar irradiance, ambient temperatures, and dust accumulation on the electrical, thermal, energy, and exergy performances of the investigated modules were evaluated. The results showed that the nanocoated PV modules performed better than the reference module and the difference in performance increased with the dust accumulation. The maximum power output of the reference module decreased to 29.50 W, whereas the TiO_2- and SiO_2-coated modules generated 35.90 W and 37.90 W, respectively, on the third day of testing. The electrical efficiency of the reference module decreased to around 10%, while the TiO_2- and SiO_2-coated modules kept efficiencies around 13% and 14%, respectively. The exergy efficiency remained higher for the coated modules throughout the experimental period. These results demonstrate that SiO_2 nanocoating is a practical, low-cost, and effective way to reduce the dust-induced performance degradation and improve the operation of the PV systems in the dusty environments.

1. Introduction

Expanding the deployment of renewable energy technologies is crucial to meet the growing energy demand while reducing environmental impacts [1]. While various types of renewable energy are used today, solar energy is the preferred option in many countries. Solar energy can be converted into thermal energy using various types of thermal collectors and into electrical energy using solar PV modules. Solar PV modules are characterized by the absence of moving parts that could malfunction, low maintenance requirements, environmental friendliness, low operating costs, and

*Corresponding Author Email: hussein.khalf@coeng.uobaghdad.edu.iq

Cite this article: Khudhur,A and Jobair,H . (2026). Experimental Study of Nanoparticles-Coated Solar Photovoltaic Modules: Energy and Exergy Enhancement. Journal of Solar Energy Research, 11(3), 3996-4010. doi: 10.22059/jser.2026.416510.1762

DOI: 10.22059/jser.2026.416510.1762

the ability to operate in remote locations to generate electrical power [2-5]. However, the widespread adoption of solar PV systems faces various obstacles due to dust accumulation and dirt on the module surfaces, in addition to the high temperature they experience when continuously exposed to solar radiation [6]. Dust reduces the amount of sunlight that the solar PV module can utilize, while increased module temperature leads to a decrease in voltage, thereby decreasing the performance of the PV system [7, 8]. Therefore, studies have focused on improving the design and arrangement of PV modules to lower the operating temperature and limit the dust accumulation on the PV module surfaces, especially in desert regions [9-11]. The combined impact of high temperature and dust accumulation critically degrades the PV module performance in these regions. Therefore, any modification should consider these factors and be simple, low-cost, and scalable for real-world applications [12-15]. Many techniques have been explored in the literature, including active and passive cooling methods [16-19], as well as mechanical and surface-based cleaning systems [20, 21].

According to Aissi et al. [22], dust accumulation affected solar PV modules made of monocrystalline, polycrystalline, and amorphous silicon, resulting in efficiency losses of 5%, 6.3%, and 14%, respectively, compared to a cleaned solar PV module. Elshazly et al. [23] indicated that high temperatures can reduce the efficiency of solar PV modules by up to 10%. They also reported that modules can lose up to half of their total efficiency after just one month without cleaning. Kareem et al. [24] evaluated the year-round performance of a solar PV system in Baghdad. The study indicated that the energy efficiency was between 15.71% and 15.74%, while the exergy efficiency varied from 10.8% to 15.8%. Nanocoating technologies have become increasingly considered an attractive and cost-effective solution to mitigate the adverse effects of dust accumulation. Nanocoating can improve the optical properties of PV surfaces by enhancing light transmittance and adding self-cleaning capabilities through the application of hydrophilic or hydrophobic effects. Moreover, nanocoating can reduce dust adhesion and facilitate particle removal, thereby maintaining a higher level of solar irradiance on the PV module surface [25-28].

Despite the growing attention to nanocoating applications, most prior investigations have focused mainly on optical or electrical performance under controlled or short-term laboratory conditions, with limited attention to comprehensive experimental evaluations under real outdoor operating conditions. In particular, there is still a lack of studies that provide a direct, side-by-side comparison of multiple nanocoating materials tested simultaneously on identical PV modules under the same real desert climate, while jointly considering electrical, thermal, energy, and exergy performance, and while tracking how this performance evolves with progressive outdoor dust exposure. The present work addresses this gap and offers the following novel contributions:

1. Direct, simultaneous field comparison of TiO_2 - and SiO_2 -coated PV modules against an uncoated reference module, tested side by side under identical real outdoor conditions in Baghdad, Iraq, rather than in a controlled laboratory or through separate, non-simultaneous trials.
2. Integrated evaluation that combines electrical, thermal, energy, and exergy performance within a single experimental framework, whereas most previous nanocoating studies report only optical or electrical results.
3. Quantification of the progressive, time-dependent effect of dust accumulation on coating effectiveness across three separate outdoor exposure days.
4. First exergy-based thermodynamic assessment of TiO_2 - and SiO_2 -coated PV modules under real dusty desert conditions, linking exergy efficiency directly to module temperature and dust accumulation rather than relying on energy efficiency alone.
5. Practical, low-cost, and scalable evaluation approach representative of harsh desert and dusty climates, providing field-based evidence to support real-world deployment decisions rather than idealized or simulated performance predictions.

The objective of the present study is to experimentally investigate the electrical and thermal performance of three solar PV modules: a conventional uncoated PV module and two nanocoated modules using TiO_2 and SiO_2 materials. The experiments were conducted under real outdoor conditions in Baghdad, Iraq, characterized by high solar irradiance, elevated temperatures, and frequent dust exposure. The analysis integrates electrical efficiency, thermal behavior, and exergy performance to a comprehensive evaluation of the investigated PV modules under dusty environmental conditions. In addition, a comparative energy enhancement evaluation was conducted to quantify the improvement attained by the nanocoated PV modules relative to the reference module under progressive outdoor exposure conditions.

2. Experimental Investigation

This section reports the experimental setup, system configuration, measurement instruments, and procedures used to evaluate the performance of the solar PV modules under real outdoor conditions.

2.1. System Configuration

The experiments were conducted under real-world outdoor conditions in Baghdad, Iraq (33.3°N 44.4°E). Three identical monocrystalline solar PV modules were investigated in this study: an uncoated reference PV module, and two coated PV modules using TiO_2 and SiO_2 nanoparticles. The arrangement of the test rig is depicted in Figure 1, with the detailed module specifications and nanoparticle properties summarized in Tables 1 and 2, respectively.

Figure 1. Experimental setup of the solar PV system (a) uncoated PV module, (b) TiO_2-coated PV module, and (c) SiO_2-coated PV module

Table 1. Specifications of the solar PV module

Parameter	Value
Open circuit voltage (V_{oc})	21.6 V
Short circuit current (I_{sc})	2.92 A
Maximum voltage (V_{mp})	18 V
Maximum current (I_{mp})	2.78 A
Maximum power (P_m)	50 W
Module efficiency	21.01%
Dimensions	63×45×2.5 cm

Figure 1 displays an experimental configuration with three identical PV modules installed in parallel. The system was positioned southward with a tilt angle of 24°, optimum for Baghdad’s sun irradiance in April [29, 30]. modules (b) and (c) were subjected to hydrophobic nanocoating treatments through a spray nozzle at a constant pressure of 0.2 MPa to impart self-cleaning capabilities. The resultant water contact angles were 139° and 152°, respectively, markedly reducing dust adherence via improved surface hydrophobicity.

Table 2. General properties of the nanoparticles

Property	TiO_2	SiO_2
Chemical composition	Rutile (30-40) wt%; Anatase (60-70) wt%	(SiO_2 -x, x = ~0.5, 99.5%), non-porous
Appearance	White nano-powder	White nano-powder
Average Particle Size (APS)	10-30 nm	20 nm
Specific Surface Area (SSA)	50-100 m²/g	160 m²/g

2.2. Experimental Procedure

The experimental work was conducted under actual climatic conditions in April 2026. The electrical parameters such as open circuit voltage, short circuit current, maximum voltage, maximum current, and maximum power output were characterized using a PV Analyzer (PROVA 210). Thermocouples were attached to the back of each PV module to record the temperature, while an additional sensor measured the ambient air temperature. All sensors were connected to a data logger for continuous recording . In addition, a solar power meter (TES-1333R) was used to measure solar irradiance. Measurements were recorded simultaneously for all PV modules from 9:00 AM to 3:00 PM at 30-minute intervals to facilitate an accurate comparative evaluation of performance. All measuring instruments were calibrated at the Organization for Standardization and Quality Control Center, Baghdad, prior to the experimental measurements to ensure the accuracy and reliability of the obtained data. The operational ranges and the respective measurement uncertainties following the calibration process are presented in Table 3.

Table 3. Calibration specifications of the measuring instruments

Instrument	Range	Uncertainty (±)
Data Logger +Thermocouple	20–80 °C	±0.08 °C
PV Analyzer (PROVA 210)	10–20 V	±0.002 – 0.006 V
Solar Power Meter (TES-1333R)	0–2000 W/m²	± 10 W/m²

Table 4 compares the measured PV parameters with the manufacturer's Standard Test Conditions (STC) specifications. The maximum power (P_{max}) and the short-circuit current (I_{sc}) shows large deviations of 19.6% and 13.2%, respectively, which can be ascribed to the difference between the outdoor spectral distribution and the controlled laboratory environment, as well as real-world operational losses. In contrast, the open-circuit voltage (V_{oc}) shows a high degree of agreement with a small error of 2.73%, indicating that the modules have sound electrical integrity and that the instrumentation and sensing framework used in this study are reliable.

Table 4. Validation of the solar PV module Electrical Parameters

Parameters	STC specifications	Measured specifications	Error %
V_{oc}	21.6 V	22.19V	2.73
I_{sc}	2.92 A	2.533A	13.2
V_{max}	18 V	16.37V	9
I_{max}	2.78 A	2.455A	11.7
P_{max}	50 W	40.18W	19.6

3. Energy and Exergy Analysis

The performance of the studied solar PV modules was investigated under actual climatic conditions by means of energy and exergy analyses. The energy analysis determined the amount of electric energy produced, while the exergy analysis measured the quality of energy conversion and reveals the thermodynamic irreversibilities in the system. The analysis was based on experimentally measured parameters, including solar irradiance (G_t), ambient temperature (T_a), PV module temperature (T_{pv}), wind speed (V_w), voltage (V), and current (I).

The ambient temperature (T_a), measured concurrently with the other operating parameters at each time step, was taken as the dead-state (reference) temperature for the thermal and exergy loss calculations, since it represents the temperature of the surroundings with which the PV module exchanges heat by convection and radiation.

As the present exergy balance considers only the radiative and convective heat exchange between the PV surface and the ambient air, rather than a working fluid or mass flow process, no dead-state pressure term appears in the formulation; the analysis was accordingly carried out at standard atmospheric pressure (101.325 kPa). All parameters (G_t, T_a, T_{pv}, V_w, V, and I) were logged at 0.5-h intervals throughout each testing day.

Because solar irradiance and ambient conditions vary continuously outdoors, the system does not operate under strict steady-state conditions; the energy and exergy balances were therefore evaluated on a quasi-steady-state basis, in which each 0.5-h interval was treated as a separate steady operating state using the average measured values recorded during that interval. This quasi-steady-state treatment is a standard assumption in outdoor field-testing of solar energy systems, since variations in solar irradiance and ambient temperature occur gradually relative to the thermal response time of the PV module.

3.1. Energy Analysis

The electrical power output of the solar PV module can be calculated as [31]:

$$P_{max} = I_{max} \times V_{max} \tag{1}$$

Where P_{max} represents the maximum power output, The electrical efficiency can be defined as [31]:

$$\eta = \frac{P_{max}}{G_t \times A_{pv}} \tag{2}$$

Where A_{pv} is the surface area of the solar PV module.

3.2. Exergy Analysis

The Petela theorem was applied to evaluate the exergy of solar radiation considering the thermodynamic limitations of the solar energy conversion. The exergy analysis evaluated the real efficiency and effective utilization of the solar PV modules. The exergy balance equation for a PV module can be expressed as [32]:

$$Ex_{in} = Ex_{out} + Ex_{loss} + Ir \quad (3)$$

Where Ex_{in} represents the input exergy, Ex_{out} represents the output exergy, and Ir represents irreversibility. Input exergy represents the total power that the solar PV modules receive from solar radiation. It can be estimated using the following formula [33]:

$$Ex_{in} = A_{pv} \times G_t \times \left[1 - \frac{4}{3}\left(\frac{T_a}{T_s}\right) + \frac{1}{3}\left(\frac{T_a}{T_s}\right)^4 \right] \quad (4)$$

Where T_s is the sun temperature which is considered as 5777 K [32]. In solar PV systems, some of the absorbed energy is lost as thermal losses by convection and radiation. The analysis must consider the important contribution of these losses to the exergy destruction. The convective heat transfer coefficient can be estimated as [34]:

$$h_{conv} = 2.8 \times 3V_w \quad (5)$$

The radiative heat transfer coefficient can be calculated as [32]:

$$h_{rad} = \varepsilon\sigma\left(T_{sky} + T_{pv}\right)\left(T_{sky}^2 + T_{pv}^2\right) \quad (6)$$

Where ε represents the emissivity of the PV module, σ represents the Stefan–Boltzmann constant, and T_{sky} represents the sky's effective temperature given by the relation:

$$T_{sky} = T_a - 6 \quad (7)$$

The total thermal exergy loss can be expressed as [35]:

$$Ex_{th} = \left(h_{conv} + h_{rad}\right) \times A_{pv} \times \left(T_a - T_{pv}\right) \times \left(1 - \frac{T_a}{T_{pv}}\right) \quad (8)$$

The output exergy is equivalent to the difference between the electrical exergy generated by the PV module and the thermal gains, which are dissipated into the environment [35].

$$Ex_{out} = Ex_{el} - Ex_{th} \quad (9)$$

Where Ex_{el} represents the electrical exergy given by equation (1). Finally, the exergy efficiency can be defined as the ratio of output exergy to input exergy [35]:

$$\eta_{ex} = \frac{Ex_{out}}{Ex_{in}} \quad (10)$$

3.3. Comparative Energy Enhancement Assessment

To investigate the effect of nanocoating on the energy performance of the PV modules, a comparative analysis of the energy improvement was conducted based on the experimentally measured power output over the three testing days. Since the electrical power varies with time due to changes in solar irradiance and operating conditions, the generated electrical energy was obtained from the measured power values during the experimental period as follows [36, 37]:

$$E = \sum_{i=1}^{n} P_i \Delta t \quad (11)$$

Where E denotes the generated electrical energy (Wh), P_i denotes the measured electrical power at each time interval (W), and Δt denotes the measurement time interval (h) equal to 0.5 h in the present study. The additional energy gain by the nanocoated PV modules was calculated by comparing the generated energy of each coated module with that of the reference module:

$$\Delta E = E_{coated} - E_{ref} \quad (12)$$

Where ΔE denotes the additional generated electrical energy (Wh), E_{coated} denotes the generated energy of the nanocoated PV module, and E_{ref} denotes the generated energy of the reference uncoated PV module. The relative enhancement in generated energy can be calculated as:

$$Enh(\%) = \frac{E_{coated} - E_{ref}}{E_{ref}} \times 100 \quad (13)$$

Where $Enh(\%)$ denotes the percentage increase in generated electrical energy due to the nanocoating application relative to the reference PV module. This comparison was adopted because all PV modules were tested under identical outdoor conditions.

4. Results and Discussion

This section presents and discusses the experimental results of the solar PV modules under real outdoor operating conditions in Baghdad, Iraq. Three PV modules were evaluated, including an uncoated reference module and two PV modules coated with TiO_2 and SiO_2 nanomaterials. The analysis focused on evaluating the effect of nanocoating on the electrical, thermal, energy, and exergy performance of the PV modules, where all investigated modules were simultaneously operated under identical environmental circumstances during each experimental day. The experimental measurements were conducted during three separate testing days with sufficient time intervals between measurements to investigate the progressive effect of dust accumulation on the electrical and thermodynamic performance of the PV modules under real outdoor operating conditions.

The findings are discussed in terms of environmental conditions, surface dust accumulation, electrical power generation, operating temperature, generated electrical energy, energy enhancement, and exergy efficiency. Figure 2 presents the variation of solar irradiance, ambient temperature, and wind speed during the experimental days. The solar irradiance values increased gradually in the morning hours and reached the maximum values around midday and then decreased gradually in the afternoon. The maximum solar irradiance values were 1009, 997, and 1014 W/m^2, on 1/4/2026, 17/4/2026, and 30/4/2026, respectively, which were recorded around 12:00–12:30 PM. The minimum solar irradiance values were recorded in the early morning and late afternoon periods. Similarly, the ambient temperature exhibited an increasing trend due to the continuous solar heating effect during the daytime.

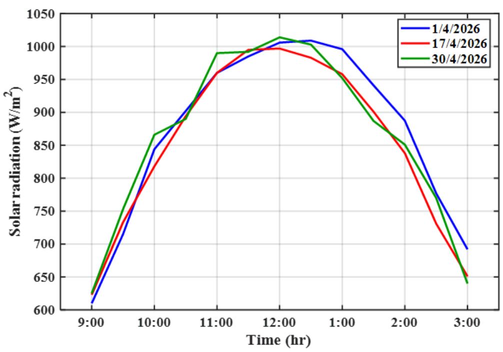

(a)

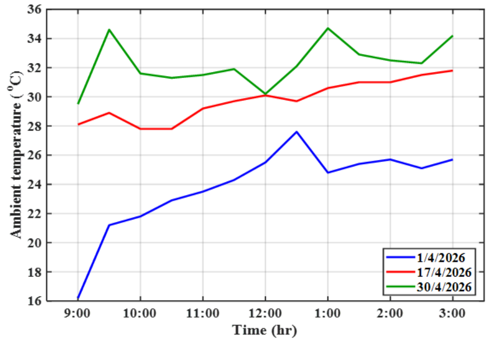

(b)

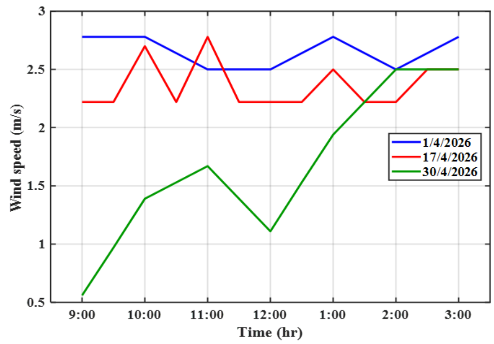

(c)

Figure 2. Distribution of (a) solar irradiance, (b) ambient temperature, and (c) wind speed during the experimental days

The maximum ambient temperature was around 27.6 °C, 31.8 °C, and 34.7 °C for the three experimental days, respectively. In addition, the recorded wind speed values varied between approximately 0.56 m/s and 2.78 m/s during the testing period, which may affect both the convective heat transfer and the dust deposition behavior on the PV module surfaces.

The power output of the solar PV modules was analyzed during the three experimental days to evaluate the effect of nanocoating on the generated power under real outdoor conditions. Since dust accumulation gradually increases with operating time and reduces the amount of solar irradiation reaching the PV surface as shown in Figure 3, comparing power output across the testing days provides a clearer understanding of the effectiveness of the applied nanocoatings.

Figure 4 shows the variation of the maximum power output with time for the reference, TiO_2-coated, and SiO_2-coated PV modules during the three experimental days. The coated PV modules generated higher power output than the uncoated reference module throughout the testing period. On the first experimental day, as shown in Figure 4(a), the difference in power output between the investigated modules was relatively small. The SiO_2-coated PV module exhibited the best performance under midday conditions, with a maximum power output of 41.15 W compared to 38.91 W for the reference module. In addition, the TiO_2-coated PV module showed a marginal increase in performance over the reference module during most of the operating hours.

Figure 3. Effect of dust accumulation on PV modules on 30/4/2026 showing the reference PV module (left), TiO_2-coated PV module (center), and SiO_2-coated PV module (right) under real operating conditions

The performance improvement was better observed for both nanocoated PV modules on the second experimental day, as shown in Figure 4(b). The maximum power output of the SiO_2-coated module reached approximately 38.77 W, and that of the TiO_2-coated module was approximately 36.96 W, against 34.95 W for the reference PV module. Such behavior indicates that the nanocoatings were useful in reducing the detrimental effects of surface contamination and in enhancing the effective use of the solar irradiation.

The most significant improvement was found on the third experimental day, as shown in Figure 4(c), when the power output difference between the coated and uncoated PV modules increased remarkably. The PV module coated with SiO_2 exhibited the highest power output during the day, reaching a peak of 37.90 W, whereas the PV module coated with TiO_2 and the reference PV module recorded 35.90 W and 29.50 W, respectively. The progressive decline in the reference module's performance over time, compared to the relatively stable output of the coated modules, indicated that the nanocoatings, especially SiO_2, provided improved anti-dust properties, higher optical transmittance, and sustained power generation under prolonged outdoor exposure.

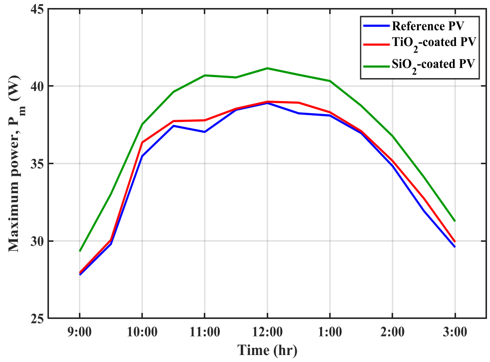

(a)

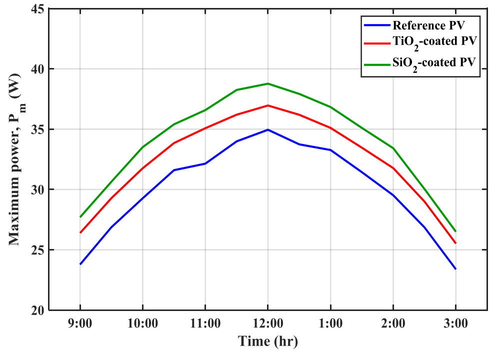

(b)

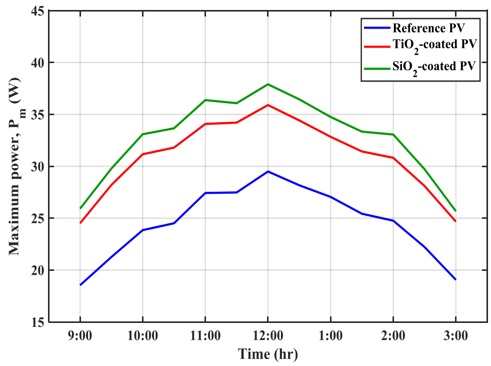

(c)

Figure 4. Variation of maximum power output with time on (a) 1/4/2026, (b) 17/4/2026, and (c) 30/4/2026

The PV conversion efficiency was evaluated for the reference, TiO_2-coated, and SiO_2-coated modules during the three experimental days in order to assess the effect of surface coating on the electrical performance under outdoor exposure. The results showed that the efficiency generally decreased during the middle hours of the day, which can be mainly attributed to the increase in module temperature under high solar irradiance. However, the coated modules maintained higher efficiency values than the reference module throughout most of the testing period, as shown in Figure 5.

On the first experimental day, the difference between the reference and TiO_2-coated module was relatively small, while the SiO_2-coated module showed a clearer improvement. The highest efficiency was about 16.08% for the reference module, 16.15% for the TiO_2-coated module, and 16.95% for the SiO_2-coated module. During the midday period, the efficiency of all PV modules decreased due to the increase in module temperature, but the SiO_2-coated module still maintained the highest efficiency.

On the second day of the experiment, the superiority of the nanocoated modules was more evident. The efficiency of the reference module was lower than that of both coated modules, especially during the high-temperature period. The TiO_2-coated module showed a significant improvement compared to the reference module, while the SiO_2-coated module attained the highest efficiency during most of the operating hours.

By the third experimental day, the difference between the coated and uncoated modules had increased further. The reference module showed the lowest efficiency, ranging from approximately 9.71% to 10.50%, while the TiO_2-coated module ranged from about 12.10% to 13.83%. The SiO_2-coated module exhibited the best overall performance, with efficiency values ranging between 12.82% and 14.63%. This behavior demonstrates that the nanocoatings, especially SiO_2, mitigated the negative effect of dust accumulation and maintained better optical and electrical performance under real outdoor operating conditions.

Figure 6 shows the variation of the operating temperatures of the reference, TiO_2 -coated and SiO_2 -coated PV modules throughout the experimental day. The temperatures of all the modules increased gradually with the rise in the solar irradiance, reaching their maximum values near the solar noon and decreasing in the afternoon. The SiO_2 -coated PV module presented the highest operating temperature, followed by the TiO_2 -coated and reference modules.

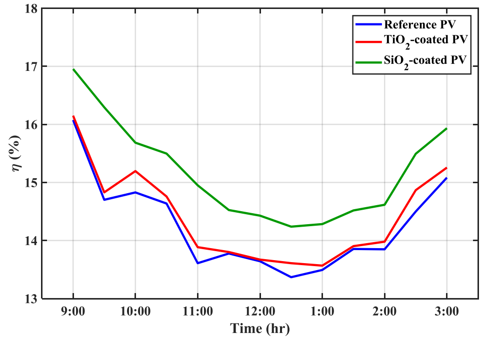

(a)

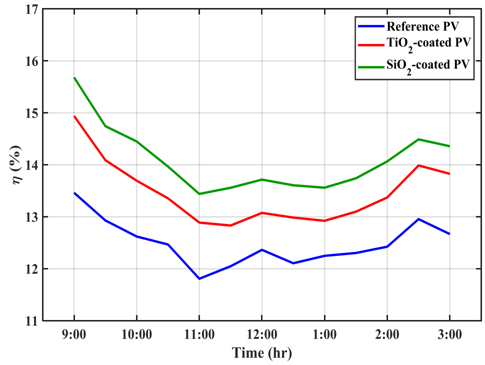

(b)

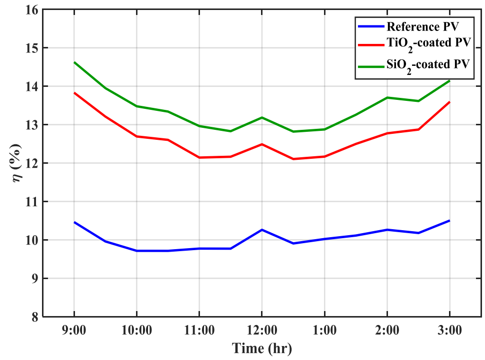

(c)

Figure 5. Variation of electrical efficiency with time on (a) 1/4/2026, (b) 17/4/2026, and (c) 30/4/2026

This behavior is mainly due to the higher optical transmittance of the SiO_2 coating, which allows a higher fraction of the incident solar radiation to be transmitted to reach the PV cells. The effect of module temperature on the electrical efficiency was examined by combining the measurements collected during the three experimental days as illustrated in Figure 7, this representation allows a better evaluation of the thermal sensitivity of each PV configuration, rather than limiting the analysis to a single day. It can be seen that the electrical efficiency decreased with the increase in PV module temperature, confirming the negative temperature dependence of the PV conversion performance. However, the reduction rate was not the same for the three PV modules. The reference PV module exhibited a significant decrease in efficiency with increasing module temperature, especially for temperatures above 45 °C. This behavior indicates that the uncoated surface was more sensitive to the combined effect of temperature increase and dust accumulation. On the other hand, the TiO_2-coated PV module showed better efficiency values in the same temperature range, suggesting that the coating mitigated part of the optical loss due to the surface contamination. The SiO_2-coated PV module showed the best overall performance, as its efficiency was higher than that of the reference and TiO_2-coated PV modules for most of the analyzed temperature range. The fitted trend lines confirm the inverse relation between the module temperature and electrical efficiency. It was observed that all the modules experienced degradation of efficiency with an increase in temperature; however, the coated PV modules, especially the SiO_2-coated PV module, showed better resistance to performance deterioration under real outdoor operating conditions. This improvement is attributed mainly to the anti-dust and optical characteristics of the nanocoating, which helped maintain better solar radiation transmission to the PV cells.

The enhancement in generated electrical energy was evaluated for the nanocoated PV modules during the three experimental days in order to assess the effectiveness of the applied coatings under progressive outdoor exposure conditions. Since the electrical power output varied continuously with solar irradiance, module temperature, and dust accumulation throughout the day, the total generated electrical energy was calculated using the measured power values over the entire operating period according to Eq. (11). The additional generated energy and the relative enhancement percentage of the coated PV modules were then determined using Eqs. (12) and (13), respectively. The results in Figure 8 indicated that both nanocoated PV modules generated higher electrical energy than the reference uncoated module during all experimental days. On the first experimental day, the improvement was relatively limited because the effect of dust accumulation was still minor. The generated energy enhancement reached approximately 1.10% for the TiO_2-coated PV module and about 6.44% for the SiO_2-coated PV module compared with the reference module.

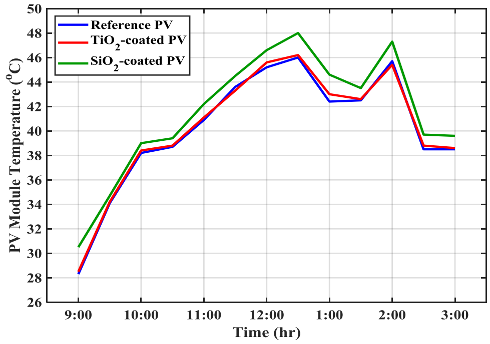

(a)

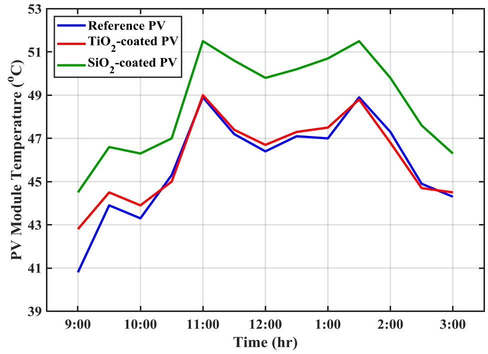

(b)

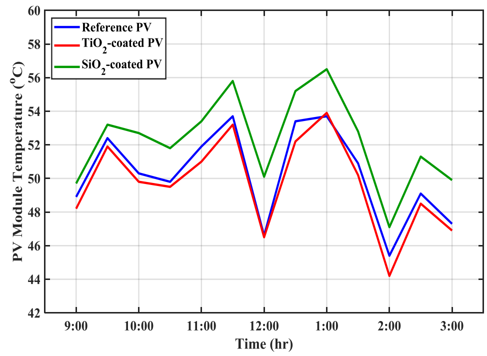

(c)

Figure 6. Variation of PV modules temperature with time on (a) 1/4/2026, (b) 17/4/2026, and (c) 30/4/2026

On the second experimental day, the influence of the nanocoatings became more pronounced, as the generated energy enhancement increased to approximately 7.62% and 12.76% for the TiO_2-coated and SiO_2-coated PV modules, respectively. This behavior indicated that coated PV surfaces had a better capability of maintaining effective solar radiation transmission as the dust exposure increased.

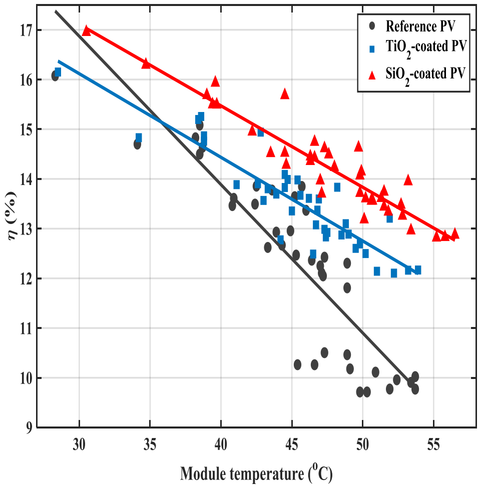

Figure 7. Effect of module temperature on the electrical efficiency of the investigated PV modules under outdoor operating conditions

The greatest improvement was recorded on the third day of the experiment, when the reference PV module showed a significant reduction in the energy generated due to the gradual accumulation of dust. On the other hand, the coated PV modules still produced higher energy throughout the operating period. The improvement in the energy generated was 25.96% for the TiO_2-coated PV module and 33.37% for the SiO_2-coated PV module. The results indicated that the nanocoatings, in particular the SiO_2 coating, significantly improved the outdoor energy performance of the PV modules under dusty environmental conditions.

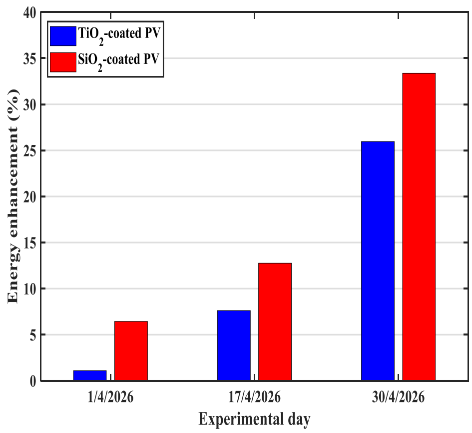

Figure 8. Comparison of generated energy enhancement for the TiO_2-coated and SiO_2-coated PV modules under progressive outdoor exposure conditions

The exergy efficiency was evaluated to provide a more realistic assessment of the useful electrical conversion performance of the investigated PV modules under outdoor operating conditions. Unlike the conventional energy efficiency, the exergy efficiency accounts for the quality of the available solar energy and therefore gives a clearer indication of the actual useful performance of each PV configuration, as shown in Figure 9.

During the first experimental day, the exergy efficiency values of the three modules were relatively close, especially between the reference and TiO_2-coated PV modules. However, the SiO_2-coated PV module generally maintained higher exergy efficiency throughout most of the testing period. The maximum exergy efficiency values were 15.92%, 15.91%, and 16.28% for the reference, TiO_2-coated, and SiO_2-coated PV modules, respectively.

The difference between coated and uncoated modules increased with the outdoor exposure time. On the second day of the experiment, the reference module showed a significant decrease in exergy efficiency, while both nanocoated modules maintained higher exergy efficiency. For most of the operating hours, the TiO_2-coated and SiO_2-coated modules showed better exergy performance than the reference module, suggesting that the nanocoatings contributed to minimizing the useful energy losses associated with dust accumulation and thermal effects.

The most significant difference was noticed on the third day of the experiment. The reference PV module was found to have the lowest exergy efficiency values, ranging from 8.61% to 10.05%, while the TiO_2-coated module ranged from 11.17% to 13.28%, and the SiO_2-coated module ranged from 11.38% to 13.52%. This confirms that the nanocoated modules, particularly the SiO_2-coated PV module, were more capable of preserving useful electrical output under progressive dust accumulation and real outdoor operating conditions.

The relationship between module temperature and exergy efficiency was examined by combining the experimental measurements collected during the three testing days. This analysis provides a thermodynamic interpretation of the PV performance because exergy efficiency reflects the useful portion of the available solar energy that is converted into electrical output. Therefore, it is more sensitive to thermal degradation and irreversibility than the conventional electrical efficiency.

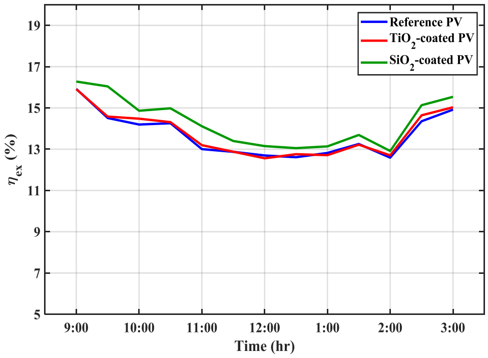

(a)

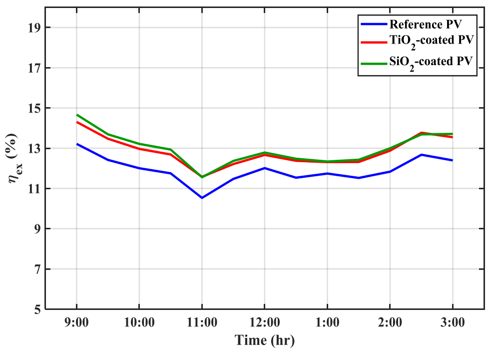

(b)

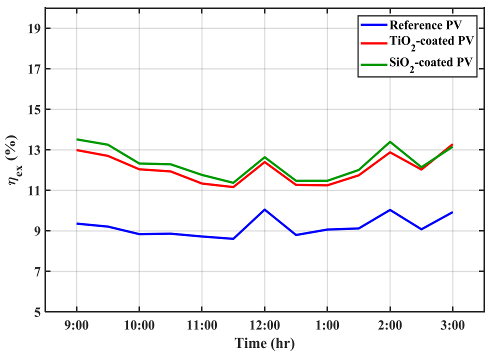

(c)

Figure 9. Variation of exergy efficiency with time on (a) 1/4/2026, (b) 17/4/2026, and (c) 30/4/2026

From Figure 10, the results showed a clear inverse relationship between module temperature and exergy efficiency. As the module temperature increased, the exergy efficiency generally decreased for all investigated PV modules. This behavior was attributed to the reduction in PV electrical output as the cell temperatures increased. Higher operating temperatures increase thermal losses and thereby reduce the useful work potential of the solar irradiation.

The maximum decrease in exergy efficiency with increasing module temperature was observed in the reference PV module. This indicated that the uncoated module was more affected by the combined influence of thermal stress and dust accumulation. At high module temperatures, particularly during the later experimental period, the reference module recorded the lowest exergy efficiency values compared with the nanocoated modules. In contrast, the TiO_2-coated and SiO_2-coated PV modules maintained higher exergy efficiency over most of the investigated temperature range. The SiO_2-coated PV module showed the best thermodynamic behavior, as its data points were mostly above the reference and TiO_2-coated modules. This suggests that the SiO_2-coating was more effective in reducing optical losses caused by dust deposition and preserving useful electrical output under real outdoor operating conditions. The fitted trend lines further confirmed the negative dependence of exergy efficiency on module temperature. Although all modules experienced exergy degradation with increasing temperature, the coated modules showed less severe performance deterioration compared with the reference PV module. This confirmed that the nanocoatings improved not only the energy output but also the quality of energy conversion under dusty and high-temperature outdoor conditions.

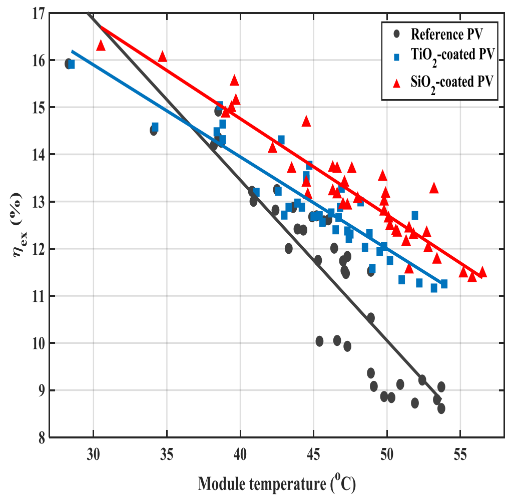

Figure 10. Relationship between module temperature and exergy efficiency for the reference, TiO_2-coated, and SiO_2-coated PV modules during the experimental period

5. Conclusions

An experimental investigation was conducted to evaluate the effect of TiO_2 and SiO_2 nanocoatings on the outdoor performance of solar PV modules under the climatic conditions of Baghdad, Iraq. Based on the obtained results, the following conclusions can be drawn:

- The nanocoated solar PV modules attained better electrical and thermodynamic performance than the uncoated reference PV module during all experimental days.
- The effect of the nanocoatings on the performance of PV modules became more pronounced with increasing outdoor exposure time due to the progressive accumulation of dust on the reference PV module surface.
- The SiO_2-coated PV module showed superior performance in terms of power output, electrical efficiency, generated energy, and exergy efficiency, compared to the TiO_2-coated and reference PV modules.
- The relative enhancement of generated energy when using TiO_2 and SiO_2 nanocoatings on solar PV modules was 25.96% and 33.37%, respectively.
- The reduced dust accumulation on the coated solar PV modules resulted in higher optical transmittance and better electrical performance compared to the uncoated PV module.
- The solar PV modules exhibited performance degradation with increasing temperature. However, the coated PV modules demonstrated better resistance to the efficiency reduction under real-world outdoor operating conditions.
- The exergy analysis indicated that the nanocoated PV modules retained a higher percentage of the available solar exergy and showed better useful energy conversion under dusty environmental conditions.
- The findings revealed that nanocoating, particularly SiO_2 coating, can be considered an effective and practical solution for enhancing solar PV system performance in desert and dusty climates.

Based on the current results, some avenues for future research are proposed. Long-term outdoor monitoring for several months or a full year is required to assess the durability and self-cleaning performance of TiO_2 and SiO_2 nanocoatings under seasonal variations of rainfall, wind, and dust loading beyond the three-day testing period considered in this study. Other or hybrid nanocoating materials (e.g. ZnO, Al_2O_3, or multilayer TiO_2/SiO_2 composites) and integration of nanocoating with active or passive cooling techniques could be explored to further reduce the temperature induced efficiency degradation. Techno-economic and environmental life-cycle assessment of nanocoating application is also needed to evaluate its cost-effectiveness for large-scale PV deployment in desert environments. Finally, expanding the experimental dataset would support the development of predictive models like machine learning-based performance forecasting for nanocoated PV systems under different dust and climate conditions.

Nomenclature

A_{pv}	Solar module surface area (m^2)
Enh(%)	Relative enhancement in generated energy (%)
E	Generated electrical energy (Wh)
Ex_{el}	Electrical exergy (kJ)
Ex_{in}	Input exergy (kJ)
Ex_{out}	Output exergy (kJ)
Ex_{th}	Thermal exergy (kJ)
G_t	Solar irradiance(W/m^2)
h_{con}	Convective heat transfer coefficient ($W/m^2.K$)
h_{rad}	Radiative heat transfer coefficient ($W/m^2.K$)
I_{max}	Maximum power output point current (Amp)
I_{sc}	Short-circuit current (Amp)
P_{max}	Maximum power output (W)
STC	Standard test condition
T_a	Ambient temperature (°C or K)
T_{pv}	PV cell temperature (°C or K)
T_s	Sun temperature (°C or K)
T_{sky}	Sky temperature (°C or K)
V_{max}	Maximum power output point voltage (V)
V_{oc}	Open-circuit voltage (V)
V_w	Wind speed (m/s)
ε	Stefan–Boltzmann constant 5.67037×10^{-8} ($W/m^2.K^4$)

η	Energy efficiency (%)
η_{ex}	Exergy efficiency (%)
σ	Emissivity of the PV module

References

[1] Abushgair, K., & Al-Waked, R. (2021). Effects of coating materials as a cleaning agent on the performance of poly-crystal PV panels. Coatings, 11(5), 544. DOI: 10.3390/coatings11050544.

[2] Luque, A., & Hegedus, S. (2011). Handbook of photovoltaic science and engineering. John Wiley & Sons.

[3] Bagher, A.M., Vahid, M.M.A., & Mohsen, M. (2015). Types of solar cells and application. American Journal of optics and Photonics, 3(5), 94-113. DOI: 10.11648/j.ajop.20150305.17.

[4] Hashemian, N., & Noorpoor, A. (2019). Assessment and multi-criteria optimization of a solar and biomass-based multi-generation system: Thermodynamic, exergoeconomic and exergoenvironmental aspects. Energy conversion and management, 195, 788-797. DOI: 10.1016/j.enconman.2019.05.039.

[5] Hashemian, N., & Noorpoor, A. (2023). Thermo-eco-environmental investigation of a newly developed solar/wind powered multi-generation plant with hydrogen and ammonia production options. Journal of Solar Energy Research, 8(4), 1728-1737. DOI: 10.22059/jser.2024.374028.1388D.

[6] Sulaiman, S.A., Singh, A.K., Mokhtar, M.M.M., & Bou-Rabee, M.A. (2014). Influence of dirt accumulation on performance of PV panels. Energy Procedia, 50, 50-56. DOI: 10.1016/j.egypro.2014.06.006.

[7] Hameed, M.A., Kaaya, I., Al-Jbori, M., Matti, Q., Scheer, R., & Gottschalg, R. (2024). Analysis and Prediction of the Performance and Reliability of PV Modules installed in harsh climates: Case study Iraq. Renewable Energy, 228, 120577. DOI: 10.1016/j.renene.2024.120577.

[8] El-Mahallawi, I., Elshazly, E., Ramadan, M., Nasser, R., Yasser, M., El-Badry, S., Elthakaby, M., Oladinrin, O.T., & Rana, M.Q. (2022). Solar pv panels-self-cleaning coating material for Egyptian climatic conditions. Sustainability, 14(17), 11001. DOI: 10.3390/su141711001.

[9] Mani, M., & Pillai, R. (2010). Impact of dust on solar photovoltaic (PV) performance: Research status, challenges and recommendations. Renewable and sustainable energy reviews, 14(9), 3124-3131. DOI: 10.1016/j.rser.2010.07.065.

[10] Qin, J., & Lu, H. (2023). A review of self-cleaning coatings for solar photovoltaic systems: theory, materials, preparation, and applications. Environmental Science and Pollution Research, 30(40), 91591-91616. DOI: 10.1007/s11356-023-28550-5.

[11] Skoplaki, E., & Palyvos, J.A. (2009). On the temperature dependence of photovoltaic module electrical performance: A review of efficiency/power correlations. Solar energy, 83(5), 614-624. DOI: 10.1016/j.solener.2008.10.008.

[12] Sayyah, A., Horenstein, M.N., & Mazumder, M.K. (2014). Energy yield loss caused by dust deposition on photovoltaic panels. Solar Energy, 107, 576-604. DOI: 10.1016/j.solener.2014.05.030.

[13] Ahmed, A., Elsakka, M., Elhenawy, Y., Amer, A., Mansi, A., Bassyouni, M., Gadalla, M., & Refaat, A. (2024). Experimental investigation of a nano coating efficiency for dust mitigation on photovoltaic panels in harsh climatic conditions. Scientific Reports, 14(1), 23013. DOI: 10.1038/s41598-024-72772-7.

[14] Fathi, M., Abderrezek, M., & Friedrich, M. (2017). Reducing dust effects on photovoltaic panels by hydrophobic coating. Clean Technologies and Environmental Policy, 19(2), 577-585. DOI: 10.1007/s10098-016-1233-9.

[15] Lu, H., & Zheng, C. (2022). Comparison of dust deposition reduction performance by super-hydrophobic and super-hydrophilic coatings for solar PV cells. Coatings, 12(4), 502. DOI: 10.3390/coatings12040502.

[16] Jobair, H.K. (2017). Improving of photovoltaic cell performance by cooling using two different types of fins. International Journal of Computer Applications, 157(5), 6-15. DOI: 10.5120/ijca2017912691.

[17] Benato, A., & Stoppato, A. (2019). An experimental investigation of a novel low-cost photovoltaic panel active cooling system. Energies, 12(8), 1448. DOI: 10.3390/en12081448.

[18] Nižetić, S., Jurčević, M., Čoko, D., & Arıcı, M. (2021). A novel and effective passive

cooling strategy for photovoltaic panel. Renewable and Sustainable Energy Reviews, 145, 111164. DOI: 10.1016/j.rser.2021.111164.

[19] Nasef, H., Nada, S., & Hassan, H. (2019). Integrative passive and active cooling system using PCM and nanofluid for thermal regulation of concentrated photovoltaic solar cells. Energy conversion and management, 199, 112065. DOI: 10.1016/j.enconman.2019.112065.

[20] Manzo, M., Maymoun, M., Qamar, R., Rihani, Y., & Al-Jahran, A. (2025). A novel solar panel self-cleaning method based on piezoelectric films. Journal of Renewable and Sustainable Energy, 17(1). DOI: 10.1063/5.0242347.

[21] Dahlioui, D., Alaoui, S.M., Laarabi, B., & Barhdadi, A. (2023). Waterless cleaning technique for photovoltaic panels on dual-axis tracker. Environmental Science and Pollution Research, 30(34), 81667-81685. DOI: 10.1007/s11356-022-23218-y.

[22] Aissi, T., Nefraoui, A., Kandoussi, K., Elotmani, R., Monkade, M., & Abouelmahjoub, Y. (2025). The impact of dust on the efficiency of various photovoltaic panels: An experimental study. Solar Energy Advances, 5, 100106. DOI: 10.1016/j.seja.2025.100106.

[23] Elshazly, E., El-Rehim, A.A., & El-Mahallawi, I. Comparison of dust and high-temperature effects on mono and poly photovoltaic panels. in IOP Conference Series: Materials Science and Engineering. 2021. IOP Publishing.

[24] Kareem, F.A., Khalaf, D.Z., Lafta, N.S., & Lateef, Y.A. (2019). Energy and exergy analysis of a solar photovoltaic performance in Baghdad. J. Mech. Eng. Res. Dev., 42(2), 44-49. DOI: 10.26480/jmerd.02.2019.44.49.

[25] Syafiq, A., Balakrishnan, V., Ali, M.S., Dhoble, S.J., Abd Rahim, N., Omar, A., & Bakar, A.H.A. (2022). Application of transparent self-cleaning coating for photovoltaic panel: a review. Current Opinion in Chemical Engineering, 36, 100801. DOI: 10.1016/j.coche.2022.100801.

[26] Rakesh Tej Kumar, K., Ramakrishna, M., & Durga Sukumar, G. (2018). A review on PV cells and nanocomposite-coated PV systems. International Journal of Energy Research, 42(7), 2305-2319. DOI: 10.1002/er.4002.

[27] Ehsan, R.M., Simon, S.P., Kinattingal, S., Kumar, K.A., & Sriharsha, T. (2022). Effects of nanocoatings on the temperature-dependent cell parameters and power generation of photovoltaic panels. Applied Nanoscience, 12(12), 3945-3962. DOI: 10.1007/s13204-022-02633-0.

[28] Rajbahadur, Y.N.K., Kumar, A., Negi, S., & Kar, S. (2024). Evaluation of hydrophobic/hydrophilic and antireflective coatings for photovoltaic panels. Journal of Coatings Technology and Research, 1-38. DOI: 10.1007/s11998-024-00929-0.

[29] Ali, F.A. (2018). Optimum tilt angle of photovoltaic panels for some Iraq cities. Journal of University of Babylon for Engineering Sciences, 26(1), 155-163. DOI.

[30] Kadhim, S.A., Al-Ghezi, M.K., & Shehab, W.Y. (2023). Optimum Orientation of Non-Tracking Solar Applications in Baghdad City. International Journal of Heat & Technology, 41(1). DOI: 10.18280/ijht.410113.

[31] Kristiyana, S., Susastriawan, A.A.P., Sudarsono, S., & Purwanto, Y. (2025). Investigation an Effect of Tilt Angle and Water Cooling on Performance of a Photovoltaic Module of a Solar-Powered Vehicle Charging Station. Journal of Solar Energy Research, 10(1), 2195-2202. DOI.

[32] Kumar, N.M., Subramaniam, U., Mathew, M., Ajitha, A., & Almakhles, D.J. (2020). Exergy analysis of thin-film solar PV module in ground-mount, floating and submerged installation methods. Case Studies in Thermal Engineering, 21, 100686. DOI: 10.1016/j.csite.2020.100686.

[33] Zuhur, S., & Ceylan, İ. (2019). Energy, Exergy and Enviroeconomic (3E) analysis of concentrated PV and thermal system in the winter application. Energy Reports, 5, 262-270. DOI: 10.1016/j.egyr.2019.02.003.

[34] Yaghoubirad, M., Azizi, N., Ahmadi, A., Zarei, Z., & Moosavian, S.F. (2022). Performance assessment of a solar PV module for different climate classifications based on energy, exergy, economic and environmental parameters. Energy Reports, 8, 15712-15728. DOI: 10.1016/j.egyr.2022.12.070.

[35] Alomar, O.R., Ali, O.M., Ali, B.M., Qader, V.S., & Ali, O.M. (2023). Energy, exergy, economical and environmental analysis of photovoltaic solar panel for fixed, single and dual axis tracking systems: An experimental and theoretical study. Case Studies in Thermal Engineering, 51, 103635. DOI: 10.1016/j.csite.2023.103635.
[36] Duffie, J.A., Beckman, W.A., & Blair, N. (2020). Solar engineering of thermal processes, photovoltaics and wind. John Wiley & Sons.
[37] Markvart, T., & Castañer, L. (2003). Practical handbook of photovoltaics: fundamentals and applications. Elsevier.